J. Phys. B: At. Mol. Opt. Phys. **33** (2000) 3307–3318. Printed in the UK PII: S0953-4075(00)50368-X

Electron capture processes in collisions between Be^{q+} ions and He atoms

S Suzuki†‡, L Gulyás†§, N Shimakura‖, P D Fainstein¶ and T Shirai†

† Japan Atomic Energy Research Institute, Tokai-mura Ibaraki, 319-1195, Japan
‡ Japan Science and Technology Corporation, Kawaguchi-shi, 332-0012, Japan
§ Institute of Nuclear Research of the Hungarian Academy of Sciences (ATOMKI), H-4001 Debrecen, PO Box 51, Hungary
‖ Graduate School of Science and Technology, Niigata University, Niigata 950-2181, Japan
¶ Comisión Nacional de Energia Atómica, Centro Atómico Bariloche, 8400 San Carlos de Bariloche (RN), Argentina

Received 24 March 2000, in final form 26 June 2000

Abstract. Theoretical calculations of the electron capture cross sections in collisions of beryllium ions with helium atoms are performed in a close-coupling method based on molecular-state expansion for the Be^{q+} ($q = 2, 4$) ion impacts below 35 keV amu^{-1}, and in the continuum distorted-wave method for the Be^{q+} ($q = 1$–4) ion impacts above 100 keV amu^{-1}. The present results are discussed in comparison with other available theoretical calculations.

1. Introduction

Since beryllium metal is one of the plasma-facing materials used in fusion reactors, beryllium ions occur as impurities in fusion plasmas where helium ions are produced through the D–T nuclear fusion reaction. Therefore, accumulation of data on helium atoms and ions in collisions with beryllium ions is strongly required, because these collisions play an important role in impurity transport phenomena and in plasma diagnostics based on charge-exchange recombination spectroscopy [1]. Charge transfer, in particular, is quite an important collision process related to helium-ash exhaust and radiative plasma cooling in edge plasmas.

To the best of our knowledge, there are no experimental data presently available for the partial (or state-selective) as well as total cross sections for electron capture in the collisions involving Be ions with He atoms. However, some theoretical calculations have been made at low and intermediate impact energies with a close-coupling technique based on the atomic-orbital (AOCC) or on the molecular-state (MOCC) expansion method: AOCC for $Be^{q+}(q = 2, 3, 4)$ ions by Fritsch and Tawara [2]; AOCC for the Be^{2+} ion by Fritsch [3] and Wang *et al* [4]; MOCC for Be^{3+} ions by Suzuki *et al* [5] and AOCC by Wang *et al* [4]; AOCC for the fully stripped Be^{4+} ion by Fritsch [6, 7], Wang *et al* [4] and Hansen and Taulbjerg [8], and MOCC by Martín *et al* [9]. At higher impact energies, on the other hand, applying the perturbative, continuum distorted-wave (CDW) approximation, only the Be^{4+} ion collisions have been discussed [10–12].

In this paper, we present the electron capture cross sections for collisions between beryllium ions and helium atoms. At collision energies below 35 keV amu^{-1}, we used the MOCC method to describe the processes with Be^{2+} and Be^{4+} ions. For these systems, preliminary MOCC calculations were already reported by Shimakura *et al* [13], where a smaller

0953-4075/00/173307+12$30.00

molecular basis set than in the present study was used. In addition, CDW calculations were performed for the collisions of $Be^{q+}(q = 1–4)$ ions in the energy range above 100 keV amu^{-1}.

2. Calculations

2.1. Molecular-state expansion method

Since the details of the present close-coupling technique based on the molecular-basis states in the adiabatic representation were presented previously by Kimura *et al* [14], here we give only a summary of the present calculations.

The electronic structures are calculated by a valence-bond configuration-interaction method with the expansion of Slater determinants where the number of active electrons is two. Slater-type orbitals (STOs) are used as a basis set in these Slater determinants.

For the (Be^{2+} + He) system, the $Be^{2+}(1s^2)$ ion is treated by a Gaussian-type model potential as follows:

$$V(r) = \sum_l V_l(r)|Y_{lm}\rangle\langle Y_{lm}| \tag{1}$$

$$V_l(r) = A_l \exp(-\xi_l r^2) - \frac{\alpha_d}{2(r^2+d^2)^2} - \frac{\alpha_q}{2(r^2+d^2)^3} - \frac{2}{r} \tag{2}$$

where r is the distance between the electron and the beryllium nucleus, the values of parameters ξ, A and d, dipole polarizability α_d and quadrupole polarizability α_q are taken from the paper by Wetmore *et al* [15].

Thirty-three configurations with 19 STOs on the beryllium ion and 19 STOs on the helium atom are used for the (Be^{2+} + He) system. For the (Be^{4+} + He) system, 68 configurations with 21 STOs on the beryllium ion and 10 STOs on the helium atom are used.

To obtain accurate energy levels for neutral helium, we include the electronic angular correlation terms, i.e. the $He(2p^2)$ configurations (and in addition, the $He(3d^2)$ configurations for the (Be^{2+} + He) system) with each optimized orbital exponent. The same technique is also employed in the calculation of the $Be^{2+}(2\ell 2\ell')$ ions. Consequently, the maximum energy deviations from the spectroscopic values [16, 17] of all molecular states for large internuclear distances become as small as 0.14% and 0.25% for the (Be^{2+} + He) system and the (Be^{4+} + He) system, respectively (see table 1).

We calculated the radial and rotational couplings with atomic-type electron translation factors (ETFs) to solve the close-coupling equations. The ETFs are included in the first order with respect to the relative velocity between both the nuclei.

The semiclassical close-coupling calculations are made in the energy range 0.1–14 keV amu^{-1} for the Be^{2+} ion collisions and 0.06–35 keV amu^{-1} for the Be^{4+} ion collisions.

Table 1. Comparison of atomic energy levels (au) in this work and other calculations for the (Be^{4+} + He) system. The values of Martín *et al* [9] are derived from figure 1(*b*) in their paper and the reading errors may be less than 0.02.

	$He(1s^2)$	$Be^{2+}(2s^2\ S)$	$Be^{2+}(2s2p)$	$Be^{2+}(2p^2\ S)$	$Be^{2+}(2p^2\ D)$
This work	−2.8994	−3.5294	−3.3127	−3.1227	−3.3304
Martín *et al*	−2.86	−3.44	−3.18[a]	[a]	−3.235
Hansen and Taulbjerg	−2.87	−3.5228	−3.2640	−3.0619	−3.4185
Spectroscopic value	−2.9034				−3.3386

[a] Not included in the close-coupling calculation of Martín *et al*.

The channels included for the (Be^{2+} + He) system are the initial $Be^{2+}(1s^2)$ + $He(1s^2)$ state and the electron captured $Be^{+}(1s^2 n\ell, n\ell = 2s, 2p, 3s, 3p, 3d)$ + $He^{+}(1s)$ states. For the (Be^{4+} + He) system, the initial Be^{4+} + $He(1s^2)$ state, the single-electron captured $Be^{3+}(2s, 2p)$ + $He^{+}(1s)$ states and the double-electron captured $Be^{2+}(2s^2\ {}^1S, 2s2p\ {}^1P, 2p^2\ {}^1S, 2p^2\ {}^1D)$ + He^{2+} states are included.

The internuclear motion is assumed to be along the straight-line trajectory for the (Be^{4+} + He) system because the charge transfer becomes probable at relatively large impact parameters. For the (Be^{2+} + He) system, the Coulomb trajectory due to the Coulomb repulsion between the Be^{2+} and the He^{2+} ions is taken into account, because the reactions at small impact parameters are dominant.

2.2. Continuum distorted-wave approximation

The CDW approximation was proposed by Chesire [18] a long time ago as a solution to the requirement set by the long-range character of the Coulomb interaction on the theoretical models describing electron capture reactions [19, 20]. In the three-body formulation of the model the initial and final unperturbed wavefunctions are distorted by continuum factors associated with the electron–projectile and electron–target interaction, respectively. An extension of the model to arbitrary projectiles and targets have been proposed by Belkić *et al* [19]. However, the main limitation of these applications lies in the introduction of an averaged Coulomb potential in determining the distortion functions. An attempt to take into account the short-range part of the interaction between the captured electron and target core was made by Bachau *et al* [21] and the importance of using more realistic interactions was demonstrated by studying the capture of an electron from a neon atom by a proton. However, as the continuum functions are represented by an expansion with Slater-type orbitals, it is not easy to extend their theory to arbitrary targets. As part of this paper, following the idea of Bachau *et al* [21], we generalized the CDW model to describe electron capture from an arbitrary target by an arbitrary ionic projectile. The extension of the model has been achieved by describing the interaction of the captured electron with the ionic projectile by means of a model potential, as in the interaction between the active electron and the target core.

Assuming that the many-electron collision can be simplified by the active-electron model, we may consider that only one electron is captured during the collision. The other electrons remain passive, frozen in their initial orbitals during the collision, and their role is taken into account as an averaged field, in which the active electron occupies its initial (φ_i) and final (φ_f) unperturbed states. This simplification allows us to calculate the transition amplitude for the active electron in the three-body formulation of the problem, which can be given as a product of two integrals:

$$T_{if}(\boldsymbol{\eta}) = -N_i \cdot N_f \cdot \boldsymbol{I}_f \cdot \boldsymbol{J}_i \tag{3}$$

where $\boldsymbol{\eta}$ is the usual transverse momentum transfer, $N_{i,f}$ are the Coulomb normalization factors, and the integrals $\boldsymbol{I}_j$ and $\boldsymbol{J}_i$ are defined by

$$\boldsymbol{I}_f = \int \mathrm{d}\boldsymbol{s} \exp(\mathrm{i}\boldsymbol{\rho}_P \cdot \boldsymbol{s}) \varphi_f^*(\boldsymbol{s}) \nabla_s \alpha_i(\boldsymbol{s}) \tag{4}$$

$$\boldsymbol{J}_i = \int \mathrm{d}\boldsymbol{x} \exp(\mathrm{i}\boldsymbol{\rho}_T \cdot \boldsymbol{x}) \alpha_f(\boldsymbol{x}) \nabla_x \varphi_i(\boldsymbol{x}) \tag{5}$$

where $\boldsymbol{x}$ and $\boldsymbol{s}$ are the position vectors of the electron with respect to the projectile and target. For definitions of the other quantities we refer to the paper by Belkić *et al* [19]. The functions α_i and α_f are related to the continuum wavefunctions ψ_i and ψ_f of the active electron moving

with velocity $\boldsymbol{v}$ in the field of the ionized target (V_i) and of the projectile (V_f), respectively, as follows:

$$N\alpha(\boldsymbol{r}) = \exp(-\mathrm{i}\boldsymbol{v}\cdot\boldsymbol{r})\psi(\boldsymbol{v},\boldsymbol{r}). \tag{6}$$

In this paper the interaction of the active electron with the target (V_i) was approximated by the Hartree–Fock–Slater model potential. At the same time, the interaction of the captured electron with the dressed projectile (V_f) was taken into account by a model potential calculated by Szydlik and Green [22] for a number of atoms and ions. So the bound ($\varphi_{i,f}$) and continuum ($\psi_{i,f}$) orbitals are obtained by the numerical solution of the one-electron eigenequation on the given $V_{i,f}$ potentials. This also requires the numerical calculation of the above integrals: $\boldsymbol{I}_f$ and $\boldsymbol{J}_i$. The latter has already been applied in the study of ionization [23]. The numerical methods applied in calculating $\boldsymbol{I}_f$ and $\boldsymbol{J}_i$ have been checked by calculating the total charge transfer cross sections,

$$\sigma_{if} = \int \mathrm{d}\boldsymbol{\eta}\left|T_{if}(\boldsymbol{\eta})\right|^2 \tag{7}$$

in H^+–$H(n_i l_i m_i) \rightarrow H(n_f l_f m_f)$–$H^+$ collisions. Numerical agreement has been obtained with the tabulated results published by Belkić *et al* [24].

3. Results and discussion

In a previous paper by Suzuki *et al* [5] the cross sections in the MOCC method were already given for the electron capture of the Be^{3+} ions in collisions with helium atoms below 10 keV amu^{-1}. In this paper we have extended the calculation to the same collision process but for the Be^{2+} and Be^{4+} ions at low energies (below 35 keV amu^{-1}). In the case of the Be^+ ion with an outer 2s electron, a similar calculation is too laborious to make, because the outer electron should be treated rigorously without any model potential. Therefore, we have not treated it here.

At high energies (above 100 keV amu^{-1}) the CDW approximation has been applied to account for all the processes involving the $Be^{q+}(q = 1\text{–}4)$ ions.

The total and partial (or state-selective) cross sections thus obtained are listed in tables 2–4.

In the following subsections 3.1 and 3.2 the present results are analysed in the low- and high-energy regions, separately, and a comparison with other available theoretical cross sections has also been made.

3.1. Low-energy collisions

3.1.1. (Be^{2+} + He) system. Figure 1 illustrates a comparison of the present results with earlier calculations of Fritsch [3] and Wang *et al* [4] for total electron capture and state-selective electron capture to the states with $n = 2$ and 3, who treated two active electrons and one active electron, respectively, in the AOCC method. We can see that these three calculations agree with each other in the overlapped energy region, although the present results are somewhat smaller than the earlier ones. In order to examine the present results in detail, we use the adiabatic potential energies for this system depicted in figure 2. The potential energy of the initial state is far below those of the final electron captured states, and there exists no apparent avoided crossing on the potential curve of the initial state. This fact means that the electron capture process can hardly occur at low collision energies. As is shown in figure 1, the cross sections decrease markedly in the energy region below 0.3 keV amu^{-1}. In the low-energy collisions, the collisions with such small impact parameters that the incident Be^{2+} ion

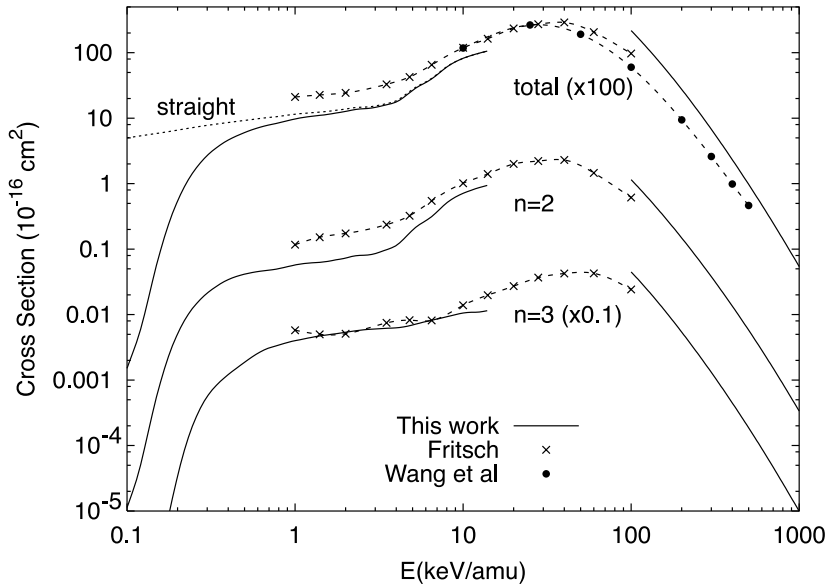

Figure 1. Electron capture cross section for the (Be^{2+} + He) system.

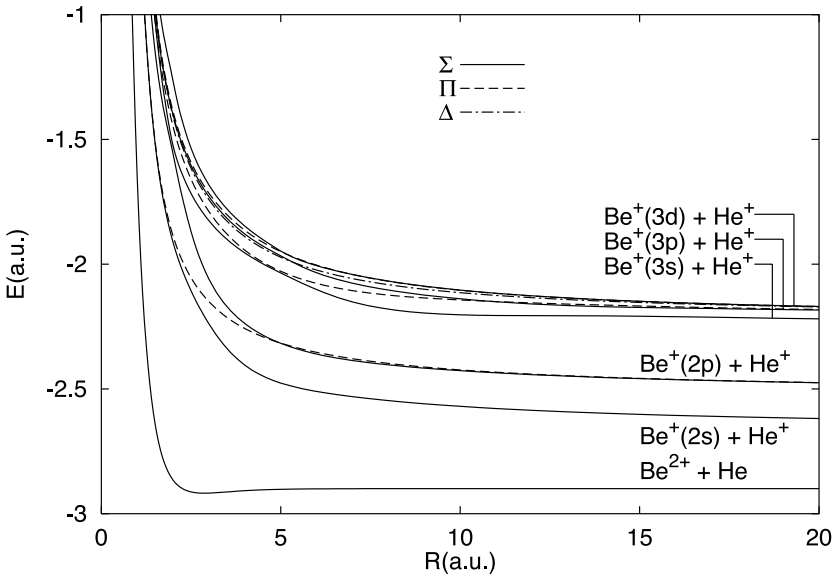

Figure 2. Adiabatic potential energies for the (Be^{2+} + He) system. All Σ, Π and Δ channels in this figure are included in the close-coupling calculations.

traverses the 1s orbital radius of the helium atom bring about the charge transfer. In these collisions, the strong Coulomb repulsive force between both the nuclei affects the trajectory of the incident ion appreciably. This trajectory effect on the cross sections is clearly seen in figure 1 in comparison between the results in the cases of a straight-line trajectory and a Coulomb trajectory.

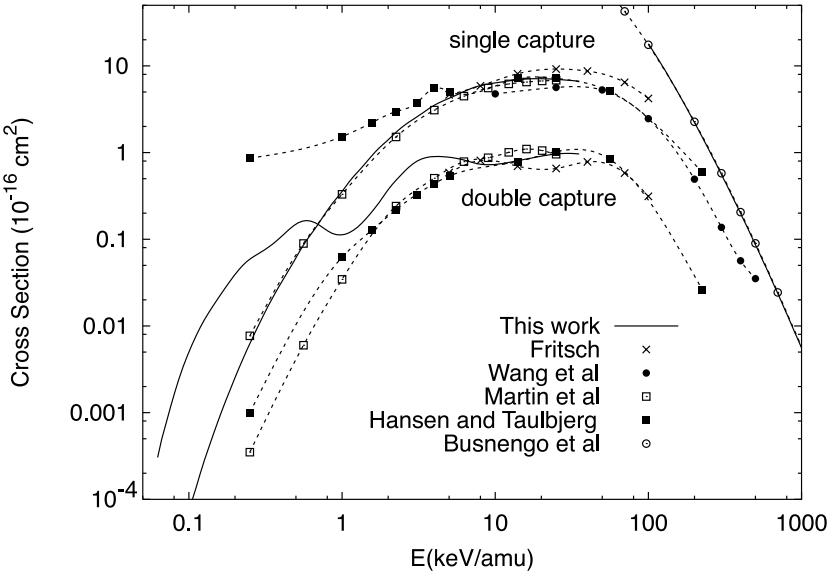

Figure 3. Electron capture cross section for the (Be^{4+} + He) system.

The cross section for electron capture to the $n = 2$ state increases rapidly in the energy range above 4 keV amu^{-1} in harmony with the earlier calculation of Fritsch [3]. This increase is due to the fact that the electron capture to the 2p state become much probable. We cannot see such an increase in the energy range above 7 keV amu^{-1} as in [3] on the cross section curve of electron capture to $n = 3$. However, both the results are generally in good agreement.

3.1.2. (Be^{4+} + He) system. The single-electron capture and double-electron capture cross sections for the (Be^{4+}+He) system are displayed in figure 3. We have included 11 MO channels in the calculation, the potential curves of which are shown in figure 4. The avoided crossing between the initial 7Σ state and the final single-electron captured state at the internuclear distance R_x has a large energy difference. On the other hand, there are some avoided crossings between the initial state and the final double-electron captured states. The energy differences at these avoided crossings are so small that we may treat them as diabatic crossings.

Figure 3 indicates that the total cross section for single-electron capture decreases monotonically with decreasing collision energy. The energy dependence comes from the fact that the energy difference of the avoided crossing at R_x is large, so that single-electron capture becomes less probable in the low-energy collisions. The present calculation is in good accord with the earlier calculations [4, 6, 8, 9] except for Hansen and Taulbjerg [8] in the energy region below 5 keV amu^{-1}. In this energy region their treatment based on an AOCC method is no longer valid. Compared with a more sophisticated calculation of Fritsch [6], who takes into account the atomic orbitals with n up to 6, all the other predictions underestimate the cross section above 10 keV amu^{-1}.

As is found in table 3, the cross sections for electron capture to the 2s and 2p states are of the same order of magnitude. This fact may be related to the Stark mixing of the 2s and 2p states of the Be^{3+} ion by the electric field of the He^+ ion. These molecular states are denoted by 1Σ and 2Σ in figure 4. The radial coupling mainly brings about the transition from the initial to the 1Σ states, because the electron cloud of the 1Σ state distributes in the direction

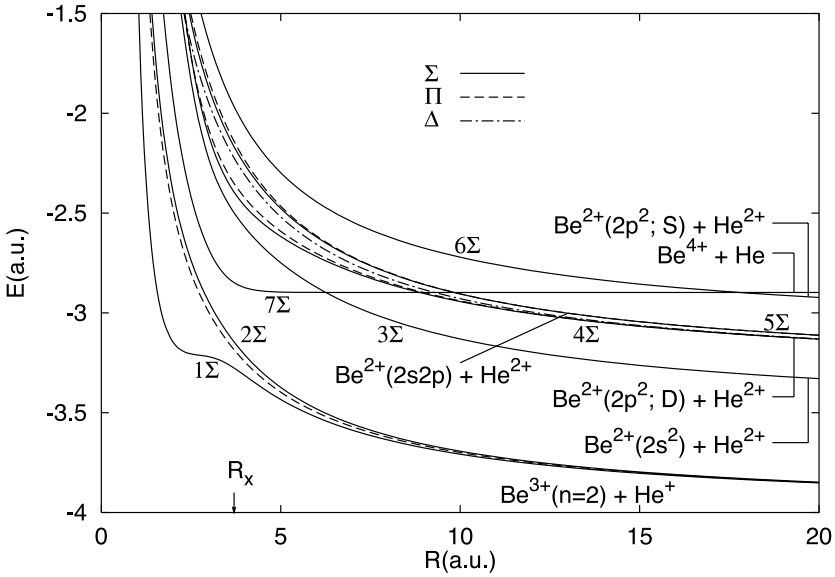

Figure 4. Adiabatic potential energies for the (Be^{4+} + He) system. All Σ, Π and Δ channels in this figure are included in the close-coupling calculations.

Table 2. Total and partial cross sections for the (Be^{2+} + H) system by the MOCC method.

Impact energy	Captured state								
(keV amu^{-1})	2s	2p	3s	3p	3d	$n = 2$	$n = 3$	Total	Straight
0.125								<1.0−4	5.44−2
0.165	<1.0−4	1.25−3[a]				1.34−3	<1.0−4	1.38−3	6.05−2
0.218	3.20−4	<1.0−4	2.71−4	2.10−4	3.09−4	7.82−3	7.89−4	8.62−3	6.81−2
0.287	9.08−4	1.84−2	1.81−3	1.33−3	1.58−3	1.93−2	4.71−3	2.41−2	7.64−2
0.379	2.99−3	2.89−2	1.54−3	6.24−3	3.03−3	3.19−2	1.08−2	4.27−2	8.43−2
0.500	4.10−3	3.74−2	1.73−3	1.20−2	4.93−3	4.14−2	1.87−2	6.02−2	9.24−2
0.758	4.52−3	4.46−2	1.12−2	5.03−3	1.68−2	4.91−2	3.29−2	8.21−2	1.05−1
1.149	1.73−2	4.33−2	9.66−3	1.03−2	2.31−2	6.05−2	4.29−2	1.04−1	1.19−1
1.999	1.57−2	5.73−2	4.36−3	2.70−2	2.25−2	7.30−2	5.37−2	1.27−1	1.38−1
3.031	9.03−3	7.72−2	2.77−3	3.78−2	1.99−2	8.62−2	6.03−2	1.47−1	1.55−1
4.000	2.74−2	8.63−2	2.67−3	4.34−2	1.71−2	1.14−1	6.29−2	1.77−1	1.84−1
4.595	5.59−2	1.01−1	3.38−3	4.65−2	1.65−2	1.57−1	6.59−2	2.23−1	2.34−1
6.064	1.22−1	1.54−1	6.58−3	5.25−2	2.10−2	2.76−1	7.86−2	3.56−1	3.63−1
8.000	2.90−1	2.20−1	1.18−2	5.42−2	2.90−2	5.11−1	9.27−2	6.06−1	6.12−1
10.556	4.17−1	3.36−1	1.72−2	5.56−2	3.81−2	7.53−1	1.08−1	8.64−1	8.60−1
13.928	5.07−1	4.33−1	2.89−2	4.92−2	4.12−2	9.41−1	1.15−1	1.06+0	1.06+0

[a] $a.bc \pm d = a.bc \times 10^{\pm d-16}$ cm^2.

toward the He^+ ion on the molecular axis. Therefore, the electron capture to the 2s and 2p states occurs with nearly equal probability.

In figure 3 we also have made a comparison between the present calculation and the earlier ones [6, 8, 9] for the total cross section for double-electron capture. In the energy region 5–30 keV amu^{-1}, all the calculations are in good accord with each other. However, we can see an oscillatory structure on our cross section curve in the region below 1 keV amu^{-1}, while

Table 3. Total and partial cross sections for (Be^{4+} + H) system by MOCC method.

Impact energy	Single capture			Double capture				
(keV amu^{-1})	2s	2p	Total	$2s^2$	2s2p	$2p^2\ ^1S$	$2p^2\ ^1D$	Total
0.0625			<1.0−4	<1.0−4	1.66−4[a]	<1.0−4	1.27−4	3.04−4
0.0949			<1.0−4	2.78−4	2.29−3	<1.0−4	1.35−3	3.97−3
0.109	<1.0−4	<1.0−4	1.19−4	8.45−4	3.84−3	1.04−4	2.28−3	7.06−3
0.144	2.75−4	2.73−4	5.48−4	4.05−3	8.75−3	2.61−4	3.97−3	1.70−2
0.190	9.75−4	1.04−3	2.01−3	1.25−2	1.76−2	3.64−4	4.25−3	3.47−2
0.250	2.92−3	3.33−3	6.25−3	2.47−2	2.52−2	8.32−4	8.10−3	5.89−2
0.330	7.45−3	9.62−3	1.71−2	3.49−2	2.94−2	1.05−3	1.54−2	8.07−2
0.436	1.70−2	2.32−2	4.02−2	5.14−2	3.39−2	2.80−3	3.45−2	1.23−1
0.575	3.90−2	5.31−2	9.21−2	7.24−2	3.54−2	4.66−3	5.19−2	1.64−1
0.758	7.78−2	1.08−1	1.86−1	4.88−2	4.65−2	3.40−3	3.56−2	1.34−1
1.000	1.48−1	2.08−1	3.56−1	3.43−2	4.97−2	1.50−3	2.70−2	1.13−1
1.319	2.64−1	3.85−1	6.48−1	4.42−2	4.80−2	1.85−3	5.41−2	1.48−1
1.741	4.47−1	6.78−1	1.12+0	9.56−2	5.22−2	1.28−3	1.15−1	2.64−1
2.297	6.96−1	1.08+0	1.77+0	1.88−1	8.60−2	2.14−3	2.21−1	4.98−1
3.031	1.00+0	1.53+0	2.53+0	2.47−1	1.10−1	3.34−3	4.22−1	7.81−1
4.000	1.37+0	2.15+0	3.51+0	2.11−1	1.28−1	3.80−3	5.58−1	9.01−1
5.279	1.71+0	2.70+0	4.41+0	1.38−1	1.81−1	7.78−3	5.46−1	8.74−1
7.431	2.21+0	3.50+0	5.71+0	8.91−2	2.27−1	2.24−2	4.15−1	7.53−1
12.500	2.71+0	4.02+0	6.74+0	1.38−1	2.47−1	5.01−2	3.39−1	7.75−1
21.022	2.99+0	4.11+0	7.11+0	2.57−1	2.59−1	5.48−2	3.54−1	9.24−1
35.355	3.11+0	3.56+0	6.67+0	3.11−1	2.66−1	4.03−2	3.46−1	9.63−1

[a] $a.bc \pm d = a.bc \times 10^{\pm d-16}$ cm^2.

the others decrease monotonically. The oscillation is due to the interference among double-electron captured states formed through strong couplings at the internuclear distance $R < 3$ au. Moreover, the present calculation predicts the cross section considerably larger than the others. Actually, Martín *et al* [9] made their MOCC calculation by taking into account five molecular states composed of the atomic states in table 1. We can see that their atomic wavefunctions are not so accurate in comparison with the present ones. Therefore, the differences mentioned above may be attributed to inaccuracy of the molecular states and to insufficiency in the number of channels involved in their MOCC calculation.

3.2. High-energy collisions

We have calculated the cross sections for total and state-selective electron capture of $Be^{q+}(q = 1–4)$ in collisions with the He atom in the energy region 100–1000 keV amu^{-1}, within the extended CDW approximation. In the approximation employed here the interactions of the active electron with the projectile and with the target both in the incoming and in the outgoing channels are represented by model potentials, in which the role of passive electrons are treated by an averaged field. This treatment gives a better description for electron capture than the original CDW approximation by Belkić [10] for a hydrogen atom target. The calculated values are listed in table 4 and plotted in figures 1 and 3 for the Be^{2+} and Be^{4+} ion, respectively. In the case of a Be^+ projectile there are no data available except for the present calculations.

In order to look into the n dependence of the state-selective cross section clearly, in figure 5 the relative contribution of different partial cross sections σ_n to the total capture cross sections σ_{tot} is plotted for the collision systems at 100 and 1000 keV amu^{-1}. Shown for comparison

Table 4. Total and partial cross sections for the ($Be^{q+}(q = 1–4) + H$) system by the CDW method. The effect of the Pauli principle, i.e. exclusion of the triplet manifold of the electron capture into 2s orbital of the Be^{+} ions and into 1s orbital of the Be^{3+} ions, is not included in this table.

Impact energy	Captured state							
(keV amu^{-1})	1s	2s	2p	$n = 2$	$n = 3$	$n = 4$	$n = 5$	Total
Be^{+}								
100		2.94−1[a]	2.50−1	5.44−1	1.17−1	4.65−2	2.46−2	7.83−1
200		4.99−2	2.93−2	7.92−2	1.68−2	6.75−3	3.43−3	1.13−1
500		2.68−3	8.29−4	3.51−3	6.52−4	2.37−4	1.12−4	4.74−3
700		7.59−4	1.84−4	9.44−4	1.70−4	6.07−5	2.85−5	1.26−3
1000		1.79−4	3.37−5	2.13−4	3.72−5	1.32−5	6.14−6	2.82−4
Be^{2+}								
100		4.26−1	7.23−1	1.15+0	4.49−1	2.10−1	1.23−1	2.18+0
200		7.51−2	7.26−2	1.48−1	5.40−2	2.62−2	1.56−2	2.75−1
500		4.02−3	1.79−3	5.81−3	1.87−3	8.11−4	4.21−4	9.78−3
700		1.13−3	3.91−4	1.52−3	4.68−4	1.99−4	1.03−4	2.50−3
1000		2.65−4	7.13−5	3.36−4	9.93−5	4.17−5	2.13−5	5.42−4
Be^{3+}								
100	1.77−1	4.89−1	2.56+0	3.05+0	1.76+0	9.44−1	5.64−1	7.66+0
200	1.53−1	1.14−1	2.61−1	3.75−1	1.92−1	1.02−1	6.09−2	1.01+0
500	2.19−2	7.11−3	6.18−3	1.33−2	5.48−3	2.63−3	1.44−3	4.77−2
700	7.84−3	2.02−3	1.29−3	3.31−3	1.27−3	5.95−4	3.22−4	1.40−2
1000	2.26−3	4.73−4	2.22−4	6.94−4	2.50−4	1.14−4	6.11−5	3.51−3
Be^{4+}								
100	1.33−1	3.85−1	4.11+0	4.49+0	4.64+0	2.98+0	1.88+0	1.80+1
200	7.48−2	1.11−1	5.94−1	7.04−1	5.30−1	3.20−1	1.95−1	2.22+0
500	1.97−2	1.07−2	1.86−2	2.93−2	1.53−2	8.09−3	4.64−3	8.66−2
700	7.94−3	3.31−3	4.09−3	7.40−3	3.48−3	1.76−3	9.91−4	2.36−2
1000	2.51−3	8.17−4	7.27−4	1.54−3	6.60−4	3.22−4	1.78−4	5.57−3

[a] $a.bc \pm d = a.bc \times 10^{\pm d-16}$ cm^2.

are the results obtained by ignoring the structure of the incident particles, i.e. by treating them as if they were bare nuclei.

It is well known that two different mechanisms govern the process. At incident energies below several hundred keV amu^{-1}, the electron is captured predominantly into a state for which the energy (E_f) is the closest to the initial one (E_i), that is, a resonant state with $E_f \simeq E_i$. For the Be^{3+} and Be^{4+} projectiles the resonant condition ($E_{\mathrm{He(1s)}} = E_{\mathrm{Be}^{q+}(n)}$) occurs principally for the $n = 2$ and 3 final levels, respectively, which is clearly seen by the dominant population of these levels at 100 keV amu^{-1} impact energy. On the other hand, as the collision energy increases up to, say, 1000 keV amu^{-1}, the momentum transfer governs the process and the dominantly populated final level is always the lowest available one. Therefore, the partial cross section is dominated by the capture of the electron into the lowest available final state.

For the lowest, $q = 1, 2$ projectile charges and for small n, the population of the different n shells conforms to the n^{-3} rule, and a shift between the n-distributions yielded by bare projectile impacts and by dressed projectile impacts is due to the fact that the $n = 1$ level is filled in the cases of Be^{+} and Be^{2+} projectiles. However, the apparent similarity of the n-distributions does not mean that the two kinds of calculations predict the cross sections to be in agreement with each other. Actually, the total cross section for the H^{+}–He collision is

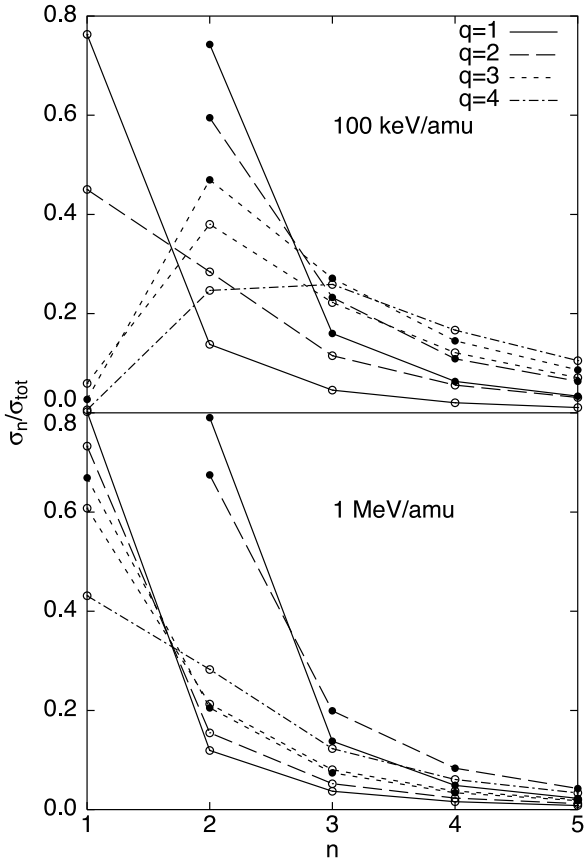

Figure 5. Ratios of the partial σ_n to the total σ_{tot} electron capture cross sections for the (Be^{q+} + He) collision systems calculated in the present CDW approximation at (*a*) 100 keV amu^{-1} and (*b*) 1 MeV amu^{-1} impact energies. The closed and open circles are from the calculations with model potential and Coulomb potential, respectively. It should be noted that the cross sections for both potentials are the same for the (Be^{4+} + He) system due to the bare projectile.

lower by an order of magnitude than that for the (Be^+ + He) system, even in the highest impact energies studied here. For the $q = 2$ projectile charge with the energy of 1 MeV amu^{-1}, both the calculations give almost the same total cross sections. However, it might be considered to be accidental, because we can find that the total cross sections for the projectile with charge $q = 3$ in these two treatments differ from each other by a factor of two. This means that the role of core electrons is not negligible in the present impact energy region, although their effect decreases with increasing charge or energy of the projectile as found by Belkić [10].

The role of core electrons is more pronounced if the population of different ℓ-sublevels in a given principal quantum number (n) is considered. The largest difference between the two kinds of calculations appears in the case of a projectile with $q = 1$. The calculation for the H^+ projectile shows that the dominantly populated level is the $\ell = 0$ level for all principal quantum numbers n. This is not the case for the Be^+ projectile, because the contribution of the $\ell = 1$ level is not negligible, especially for the $n = 2$ and 3 levels. This effect might stem from the fact that the region of collision is slightly extended to larger impact parameters if the electronic structure of the projectile is included in the calculation [25]. With increasing impact

energy or charge of the projectile ion the difference diminishes and both calculations predict similar relative populations on the sub-shells.

Owing to some general limitations, the lowest energy at which the CDW model still predicts reliable cross sections, is at around 100 keV amu^{-1} (it is slightly lower (higher) for smaller (larger) projectile charges). In figures 1 and 3 the present CDW cross sections are illustrated in comparison with the two-electron AOCC calculations of Fritsch [3, 6] and the one-electron-AOCC calculations of Wang *et al* [4] for the $Be^{2+,4+}$ projectiles. From the comparison one might conclude that the present CDW cross sections become reliable at energies above 200 keV amu^{-1}, because the deviation from the most sophisticated AOCC predictions of Fritsch diminishes in the energy region. As is shown in figure 3 the present CDW cross section for the (Be^{4+}+He) system is in good agreement with CDW-EFS (eikonal final-state) calculation of Busnengo *et al* [11].

Conclusion

We have applied the MOCC theory for low-energy collisions and the CDW approximation for high-energy collisions, to investigate the cross sections for electron transfer in (Be^{q+} + He) ($q = 1$–4) collision systems. In the previous work published so far, the mechanism was mostly analysed in the AOCC theory at intermediate energies, where the cross sections became large or reach the maximum. The present results connect or are in good agreement with them at the overlapped energy ranges. As shown in this paper, a combination of the MOCC, AOCC and CDW calculations provides reliable total and state-selective cross sections for charge transfer over a wide energy range covering the requirements from various applications including fusion reactor development. At low energies, however, there appears to be an intriguing oscillatory structure on the curve of the double-electron capture cross section. In order to assess the treatments used in the present study, however, comparison of the present results with experimental measurements is an excellent method. However, data accumulation for the collision processes studied here is as yet very limited.

Acknowledgments

We would like to express our thanks to Dr M Nakagawa and Dr A Hasegawa of the Japan Atomic Energy Research Institute for their encouragement during this work. This work was partially supported by the STA Research fellowship programme of the Science and Technology Agency of Japan. LG and PDF acknowledge financial support from the International Atomic Energy Agency (contract no 10084/RO) and from the Hungarian–Argentinean Intergovernmental S&T Cooperation Programme (SCyT-OMFB HUN4/99/OG). LG gratefully acknowledges the grant provided to him from the J Bolyai Research Scholarship.

References

[1] Suzuki S, Shimizu K, Kubo H, Shirai T, Sakasai A, Sugie T and Asakura N 1999 *Europhys. Conf. Abstracts 23J (26th EPS Conf. on Controlled Fusion and Plasma Physics (Maastricht))* p 477
[2] Fritsch W and Tawara H 1996 *National Institute for Fusion Science Report* NIFS-DATA-39 Nagoya, Japan p 89
[3] Fritsch W 1996 *Phys. Scr.* T **62** 59
[4] Wang Y D, Toshima N and Lin C D 1996 *Phys. Scr.* T **62** 63
[5] Suzuki S, Shimakura N, Shirai T and Kimura M 1998 *J. Phys. B: At. Mol. Opt. Phys.* **31** 1741
[6] Fritsch W 1995 *Nucl. Instrum. Methods* B **98** 246
[7] Fritsch W 1997 *Phys. Scr.* T **73** 197
[8] Hansen J P and Taulbjerg K 1993 *Phys. Rev.* A **47** 2987

[9] Martín F, Riera A and Yáñez 1985 *Phys. Rev.* A **34** 4675
[10] Belkić Dž 1991 *Phys. Scr.* **43** 561
[11] Busnengo H F, Corchs S E, Martínez A E and Rivarola R D 1996 *Phys. Scr.* T **62** 88
[12] Busnengo H F, Martínez A E and Rivarola R D 1995 *Phys. Scr.* **51** 190
[13] Shimakura N, Suzuki S, Murakami Y, Gu J P, Hirsch G, Buenker R J, Kimura M and Shimamura I 1996 *Phys. Scr.* T **62** 39
[14] Kimura M, Sato H and Olson R E 1983 *Phys. Rev.* A **28** 2085
[15] Wetmore A E, Cole H R and Olson R E 1986 *J. Phys.* B **19** 1515
[16] Bashkin S and Stoner J R Jr 1975 *Atomic Energy Levels and Grotrian Diagrams* vol I (Amsterdam: North-Holland)
[17] Kelly R L 1987 *J. Phys. Chem. Ref. Data* **16** *Suppl.* no 1
[18] Chesire I M 1964 *Proc. Phys. Soc.* **84** 89
[19] Belkić Dž, Gayet R and Salin A 1979 *Phys. Rep.* **56** 249
[20] Dewangan D P and Eichler J 1994 *Phys. Rep.* **247** 59
[21] Bachau H, Deco R and Salin A 1988 *J. Phys. B: At. Mol. Opt. Phys.* **21** 1403
[22] Szydlik P P and Green A E S 1974 *Phys. Rev.* A **9** 1885
[23] Gulyás L, Fainstein P D and Salin A 1995 *J. Phys. B: At. Mol. Opt. Phys.* **28** 245
[24] Belkić Dž, Gayet R and Salin A 1992 *At. Data Nucl. Data Tables* **51** 59
[25] Janev R K, Presnyakov L P and Shevelko V P 1985 *Physics of Highly Charged ions (Springer Series in Electrophysics vol 13)* (Berlin: Springer)